A fast and accurate image-based measuring system for isotropic reflection materials

Duck Bong Kim[a], Kang Yeon Kim[a], Kang Su Park[a], Myoung Kook Seo[a], Kwan H. Lee[*a]

[a] Intelligent Design and Graphics Laboratory
Department of Mechatronics, Gwangju Institute of Science and Technology (GIST)
1 Oryong-dong, Puk-gu, Gwangju, 500-712, South Korea

ABSTRACT

We present a novel image-based BRDF (Bidirectional Reflectance Distribution Function) measurement system for materials that have isotropic reflectance properties. Our proposed system is fast due to simple set up and automated operations. It also provides a wide angular coverage and noise reduction capability so that it achieves accuracy that is needed for computer graphics applications. We test the uniformity and constancy of the light source and the reciprocity of the measurement system. We perform a photometric calibration of HDR (High Dynamic Range) camera to recover an accurate radiance map from each HDR image. We verify our proposed system by comparing it with a previous image-based BRDF measurement system. We demonstrate the efficiency and accuracy of our proposed system by generating photorealistic images of the measured BRDF data that include glossy blue, green plastics, gold coated metal and gold metallic paints.

Keywords: BRDF acquisition, Image-based system, Isotropic material, High Dynamic Range Camera, Photorealism

1. INTRODUCTION

Measuring of light reflection from a given surface is one of important areas in computer graphics[1]. Measured BRDF (Bidirectional Reflectance Distribution Function) data enables us to generate photorealistic images so that it can be used for many image analysis tasks. It can be used to validate reflectance models for particular materials. The BRDF[2] describes how light reflects on a given surface point. A general BRDF describes reflected radiance as a four dimensional function that consists of two incoming and two outgoing directions. In this study we focus on isotropic BRDF, in which the rotation angle of incoming and outgoing directions about the surface normal is fixed. The isotropic BRDF data can be described by a three dimensional function of the incoming angle from the surface normal and the reflected radiance over the entire hemisphere.

Little work has been done concerning the measurement of BRDFs compared to establishing a BRDF model such as Phong[3], Blinn-Phong[4], Cook-Torrance[5] and HTSG[6]. Traditionally, BRDF data is measured using gonio-reflectometers-based system[7-10]. These systems require three to four angular dimensions to position a light source and a detector that cover all directions for a flat target sample. However, the BRDF acquisition easily takes more than several hours to move the rotary stage and measure the reflected light for each direction. Many researchers[11-20] have attempted to make this acquisition process more efficient. The technological advance of image sensor arrays such as CCD enables them to reduce the acquisition time. However, it still requires taking multiple HDR (high dynamic range) images at each direction and this leads to a long acquisition time. The post-processing of the huge amount of raw image data adds more computation as well.

In this study, we present a system that measures the BRDF data with high speed and accuracy. Our proposed system acquires a radiance map using a HDR (High Dynamic Range) camera [18]. The HDR camera captures the light reflected from many different orientation of a part of using a spherical sample. The BRDF is determined by considering the geometric shape of spherical sample and the position of the light source and the detector. The main strength of using the HDR camera is to acquire a highly dense BRDF sample without taking multiple images at one orientation, while is the

* To whom correspondence should be made: khlee@gist.ac.kr

Reflection, Scattering, and Diffraction from Surfaces, edited by Zu-Han Gu,
Leonard M. Hanssen, Proc. of SPIE Vol. 7065, 70650I, (2008)
0277-786X/08/$18 · doi: 10.1117/12.793970

case for using a LDR (Low Dynamic Range) camera. The HDR camera can acquire approximately 8 orders of luminance magnitude at once while the LDR camera[17-20] requires taking 12 to 18 images in order to recover the radiance map from multiple exposure images. Our proposed system provides us dense and accurate BRDF samples that cover the hemisphere to near grazing angles with the speed much faster than LDR camera based systems.

2. BACKGROUND AND PREVIOUS WORK

There are mainly four types of BRDF measuring systems. The gonio-reflectometer-based system[7-10] is composed of a light source, a detector, a gonio-reflectometer that gives three to four degrees of freedom, and a fixed for a flat sample. The mirror-based systems[11, 12, 13] consist of a curved mirror and a detector such as a CCD sensor. Some systems use multiple light sources and detector[14, 15]. There also exist image-based BRDF measurement systems [16-20] that use a CCD sensor and a fixture for a spherical sample. Each type of devices has its own strengths and limitations, as illustrated in Table 1.

H. Li et al.[10] developed a gonio-reflectometer based system which measures the BRDF from a flat sample that has an isotropic reflectance property. The system has a broad angular coverage and also can measure the entire visible spectrum with ample wavelength resolution. It can measure real materials in less than 10 hours and satisfies accuracy that is needed for computer graphics applications. The angular coverage includes the entire incident and reflection hemisphere to an angle of 85degree with the exception of 7 degree around retro-reflection. But the system does generate dense BRDF samples for the given material. It takes a long time to acquire BRDF data.

The technological advances of image sensors such as CCD enable us to reduce the BRDF acquisition time. The array sensor can measure a two dimensional range of angles simultaneously. Using the CCD sensor, Ward[11] developed an image-based system using a curved mirror and a fish-eye lens that gathers light scattered from a flat sample. This system is efficient since the camera captures the BRDF data at once. However, this system is limited by the use of a semi-silvered mirror which only approximates the ideal ellipsoid. Moreover the vignetting effect generated by using the ellipsoidal mirror and the fish-eye lens limits the quality of measurements near the grazing angle.

Dome type systems[14,15] that consist of multiple light sources and detectors have been developed for a fast and high quality BRDF measurement. These systems can acquire the BRDF data within a very short time, and no moving parts are required to operate the system. But the angular resolution of these systems depends on the number of light sources and detectors, so that it takes to build an expensive and bulky system to acquire highly dense BRDF data. It is also reported that synchronizing and parallel processing of each light source and detector becomes a challenging task. Recently a small dome type BRDF measurement system[15] has been developed that uses LEDs (Light Emitting Diodes) as both light detectors and light emitters. Although this system provides very rapid operation, the accuracy is limited due to the low angular resolution and unwanted light reflected from the dome.

Marschner[17] developed an efficient image-based measurement system that used a digital camera and a spherical sample. Inspired by his work, many researchers constructed image-based measurement systems[18,19,20] to measure isotropic materials. A fixed camera takes the images of the material sample under varying illumination with an orbiting light source. These image-based measurement systems have become popular due to a simple system setup, high accuracy and relatively quick acquisition time. However, it requires generating high dynamic range images at each direction to acquire BRDF data, and this leads to a long acquisition time. It also generates a huge amount of raw data which easily reaches more than 4 GB.

Our proposed system uses a hardware configuration similar to Marschner's and Matusik's image-based measurement systems except for using a HDR camera instead of using a LDR camera. We made improvement over the previous systems by using a specially designed light source module and a HDR camera as a detector module. Our proposed system is fast due to simple set up and automated operations. It also provides a wide angular coverage and noise reduction capability so that it achieves accuracy that is needed for computer graphics applications. The comparison between our proposed system and previous BRDF measurement systems are shown in Table 1.

Table. 1 Comparison between BRDF measurement systems

System	Rapid operation		Accuracy			Simple system setup
	Acquisition time	Little post-processing time	Broad angular coverage	Sampling resolution	Noise reduction	
Gonio-reflectometer[7,8,9,10]		○	○		○	
Mirror-based[11,12,13]	Δ	Δ				
Multiple setup[14,15]	○	○	○		Δ	
LDR-based[16,17,18,19,20]	Δ	Δ	○	○	Δ	○
Our proposed HDR-based	○	○	○	○	○	○

3. IMAGE-BASED BRDF MEASUREMENT SYSTEM SETUP

Our proposed system consists of four modules as shown in Fig. 1: a light source, a detector, a fixture for the material sample and a control module. A very bright light source that provides directional light is used to illuminate the material sample. We use a HDR camera[21] as a detector module since we can directly estimate the luminance from the HDR images. We also have a spherical isotropic material sample engaged at the fixture. Finally, the control module automatically performs data acquisition and post processing of data while rotating the light source.

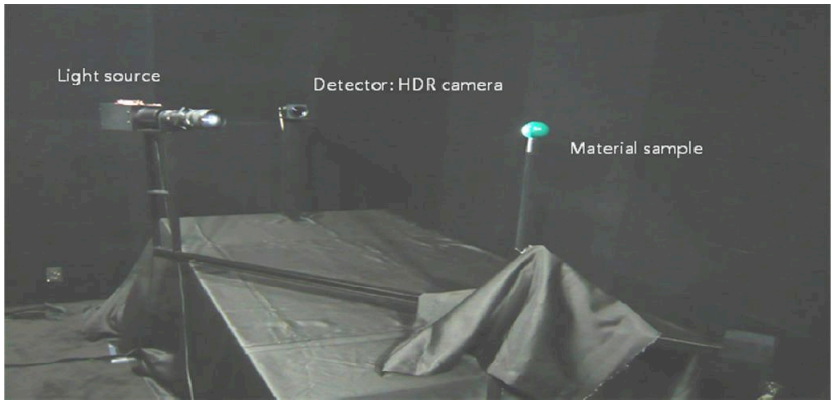

Fig. 1 Our proposed image-based BRDF measurement system

3.1. Light source module

The ideal condition for the light source would be uniform emission across the wavelength from 400 to 700 nm and be collimated and unpolarized. We used the design similar to Li's light source module[10], as shown in Fig. 2. The weight of the light source module must be light so that the arm that holds the light source module does not bend during operation. The module must not generate excessive heat which may deteriorate the other components of the module. Considering all these requirements, we chose a metal halide lamp (OSRAM POWERSTAR HQI-R 150W) with an integral dichroic reflector. Previous studies used [16-20] tungsten lamp, xenon arc lamp or LED as the light source. The light source provides a continuous spectrum in the desired range while minimizing infrared emission and reducing heat for safety. To eliminate residual polarization from the light source, we used a holographic diffuser. The beam is gathered by an aspheric condenser lens and passed through a small aperture to approximate a point light source, and then collimated by a Nikon camera lens (f =85 mm 1.4). We attached the Hoya 80B color filter in front of the Nikon camera lens to increase the color temperature of our light source from 4200 K to 5840 K. Fig. 2 (right) shows the illuminated area by our light source on the Spectralon white reference. We verified our light source module by testing the uniformity and checking optical properties' constancy.

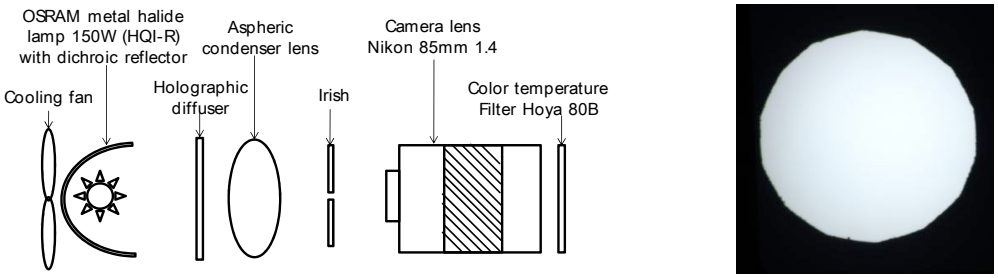

Fig. 2 Light source optical components (left) and illuminated area on the Spectralon white reference (right)

3.1.1. Uniformity check

We check the uniformity of our light source by photographing a Spectralon white surface illuminated by our light source using a scientific grade charge-coupled device (Q-Imaging). We restrict our illuminated size that has the diameter of 80 mm to increase the angular coverage. If the illuminated size is larger, the angular coverage becomes smaller since the bigger illuminated area can directly illuminate the HDR camera and generate noises such as glare and ghost effect. Fig. 3 shows the uniformity of each R, G, B channel, which is within ± 3% over a 60 mm diameter circular region.

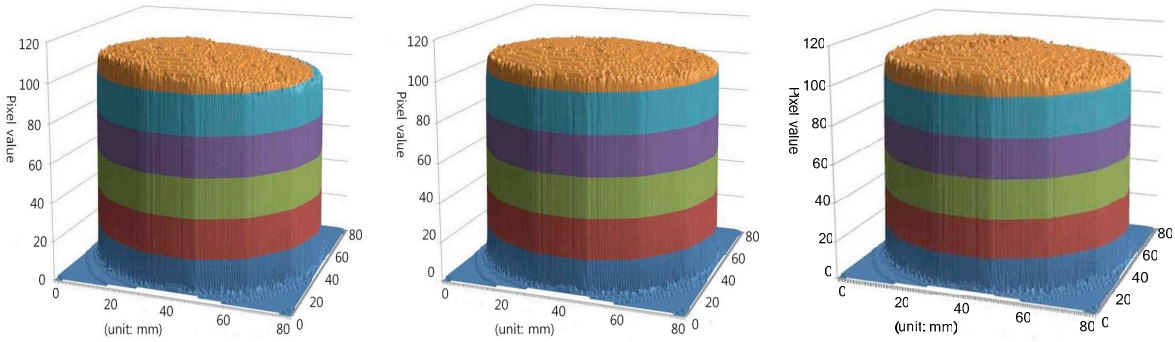

Fig. 3 Uniformity of red channel (left), uniformity of green channel(center), uniformity of blue channel (right)

3.1.2. Constancy over the time

The light source is powered by an OSRAM POWERTRONICS PTU 150 regulator that gives a stable output in illuminating the target sample. To check the luminous flux, correlated color temperature and color rendering index over time, we used ISP500-100 integrating sphere by Instrument systems. As shown in Fig. 4, we can observe that the light properties such as the luminous flux, correlated color temperature, and color rendering index become stable three minutes after the light is turned on. We therefore use the BRDF data of each material after the lapse of three minutes.

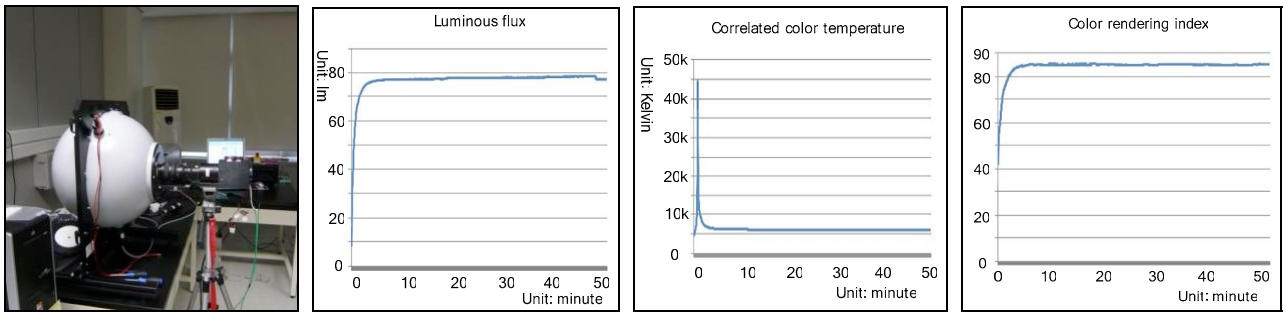

Fig. 4 Light property constancy check over time, (left) experimental setup for light source properties check, (center left) luminous flux, (center right) correlated color temperature, and (right) color rendering index

3.2. Detector module

Recently many researchers [18,19,20,22] have tried to recover a radiance map from the HDR images. Three different methods exist to acquire HDR images. The first method generates an HDR image based on multiple acquisition of the target scene using different exposure settings[22]. They[17-20] use a LDR camera, but takes several multi-exposure images which takes 5 to 30 seconds for each light source position. It usually generates a huge amount of data, for example 4 GB of data for the case of Matusik's. It is time consuming to acquire the BRDF data and to handle the raw data for post-processing. The second method [23] collects the charge generated by the photo current. The amount of charge collected per unit of time is linearly related to the irradiance on the chip, but the exposure time varies per pixel. This method is also time-consuming to acquire the BRDF data; furthermore, the accuracy is limited, as referred in Krawczyk's technical paper[24]. The third method uses the logarithmic response of a component to compute the logarithm of the irradiance in the analog domain. In recent years, HDR image sensors[21] based on CMOS technology have been developed that are capable of capturing images with a dynamic range of up to 8 orders of magnitude at video frame rates. For our detector module, we use this method which enables us to dramatically reduce the acquisition time for the BRDF acquisition.

Our detector module consists of a HDR camera[21] manufactured by IMS-Chips system and Edmund zoom manual video lens. The full resolution of the HDR camera is 640*480 pixels. The distance from the HDR camera to the target sample is 2 meters. The spherical material sample has the diameter of 60 mm. We used a CCD video zoom lens in order to use the full resolution of the HDR camera. We can reduce the acquisition time by using this HDR camera. The pixel values from the HDR camera range from 0 to 4096 for each R, G, B channel, in contrast to those of 0 to 256 from the LDR camera. A typical exposure time is 30 ms for each 0.1 degree angular configuration, resulting in the measurement time of 90 seconds for entire data acquisition that includes about 169 degree angular span.

3.3. Material sample

Our acquisition system requires a spherical shape material sample. We prepared four material samples having isotropic reflectance property and having different colors and/or surface characteristics that include glossy blue, green plastics, gold coated metal and gold metallic paints, as shown in Fig. 8. For the gold material sample, we used a steel bearing ball, and deposited a pure gold coating on the surface by a professional coating company. A gold metallic paint is also coated uniformly and spotlessly.

3.4. Automatic control acquisition

The control module performs automatic acquisition of data. It rotates the light source module and performs post processing of data. During acquisition, the light source moves in an increment of 0.1 degree from 3.5 degree to 173 degree using an accurate rotary stage (Suruga Seiki KS402-180) controlled by this module. For each position, we take one HDR image which can be generated less than 30ms. The raw HDR image data acquired by the HDR camera for each orientation is 950 KB. Consequently, it takes approximately 90 seconds to measure the whole BRDF of a material sample and generates the raw data of about 162 MB for one degree incremental step. It gives a significant data reduction compared to traditional image-based BRDF measurement systems[17-20] which often produce several Giga bytes of data.

4. NOISE REDUCTION AND CALIBRATIONS

4.1. Noise reduction

Noise reduction and calibration are essential in accurate measurement of the BRDF. We built a dark room for measurement and also performed noise reduction of the acquired data. The geometric and photometric calibrations are also performed to produce accurate data.

4.1.1. The dark room

For measurement, we built a dark room[25] where the material is actually measured and another room where a control computer is located. In the dark room, the light reflecting from the walls, the floor and the ceiling must not illuminate the material sample. The stray light must be absorbed and reflected in a diffuse way as much as possible. We constructed a small prefabricated building as a dark room taking an area of about 24 m^2. The walls and the ceiling are covered with high quality blackout papers[26] which are coated with fine, randomly oriented fibers. We use a black needle fleece carpet

for the floor. For optical stability and detector's constancy, air conditioning is provided to maintain the dark room at 20℃ and a relative humidity of 50%. The optical table is covered with black curtain and the HDR camera, the fixture for the spherical material sample and the light source arm are also covered with the blackout papers. Fig. 1 shows our dark room for BRDF measurement.

4.1.2. Noise reduction of the HDR images

As described in Krawczyk's paper[24], the HDR camera has problems in a dark condition which causes fixed pattern noise in the sensors. Due to the heating of the CMOS sensor, statistical variation occurs for a number of thermally generated electrons. To reduce this noise, we perform a FPN (Fixed pattern noise) correction. Firstly, we acquire ten HDR images in a complete dark environment. From the ten HDR images, we generate the first mean value of these images and obtain the second mean value for each pixel using ten HDR images for each channel of R, G, B. Ideally the second mean value should be the same, but a small difference of -7 to 8 pixel value between neighboring pixels occurs due to the fixed pattern noise. We consider this difference as the noise level. We generate a mean noise image by subtracting the second mean value from the first mean value. Finally, we can acquire noise reduced HDR images by adding the mean noise image for every newly recorded HDR image.

4.2. Geometric calibration

We establish a geometric relationship between the HDR camera, the sample and the light source using Tsai's camera calibration method[27]. First, we manually set up the light source, the digital camera, and the sample to the designated positions using a micrometer gauge. We then iteratively translate and rotate the HDR camera to align the center of the sample with the optical axis of the camera. In order to increase the geometric accuracy, we position the HDR camera and the light source apart from the material sample as much as possible.

4.3. Photometric calibration of high dynamic range camera

For the photometric calibration of a high dynamic range camera, we determine the camera response curve using a method based on the Krawczyk's absolute calibration [24]. This method describes the relationship between pixel values in CMOS sensors and their corresponding intensity values.

4.3.1. Experimental setup

In order to perform absolute photometric calibration of a HDR camera, we prepare an experimental setup that includes a color checker, a light source, a HDR camera and a chromameter (Konica Minolta CS-200) which measures luminance and chromaticity, as shown in Fig. 5 (left). In order to generate different illumination condition, we attach a neural density filter with ND2, ND4 or ND8 extension factor in front of Nikon lens. In addition, we acquire the light directly from the light source towards the HDR camera and the chromameter to obtain a sufficient number of samples in the upper dynamic range, as shown in Fig. 5 (right). We acquired 36 samples using a color checker and 9 samples using the direct measurement from the light source, respectively.

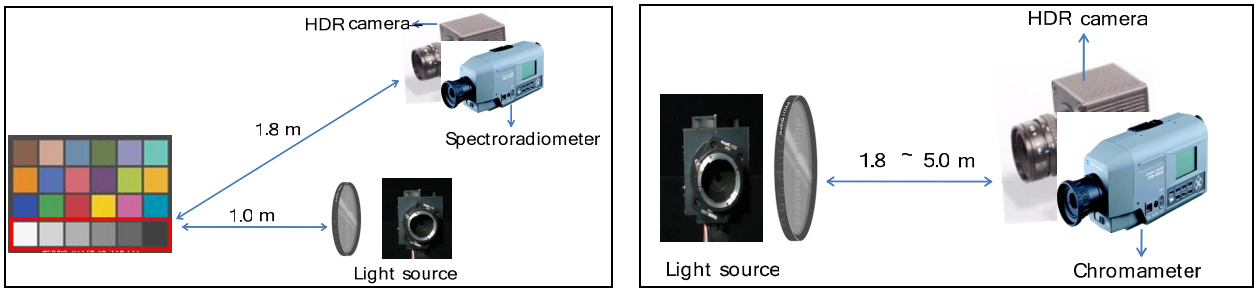

Fig. 5 Experimental setup for absolute photometric calibration of high dynamic range camera: (left) experimental setup for lower and middle dynamic ranges, (right) experimental setup for upper dynamic range

4.3.2. Absolute calibration

The absolute calibration should be separately determined for each R, G, B channel since the color channels are not identical. The chromameter gives us the luminance (Y) and chromaticity (x,y) of 45 samples. We convert these values to the CIE tri-stimulus XYZ[31]. And we convert the XYZ value into RGB absolute values using sRGB transform matrix. We then fit the HDR camera output values directly to the measured luminance and chromaticity values from the experiment.

For the HDR camera, we fit the parameters of a logarithmic function $y_i = a * log_{10}(x_i) + b$ for each channel of R, G, B using a least-square fitting algorithm. Fig. 6 shows the fitted results which show the constants a and b for each channel of R, G, B. Finally, we can determine the absolute response curve for each channel of R, G, B using three logarithmic functions.

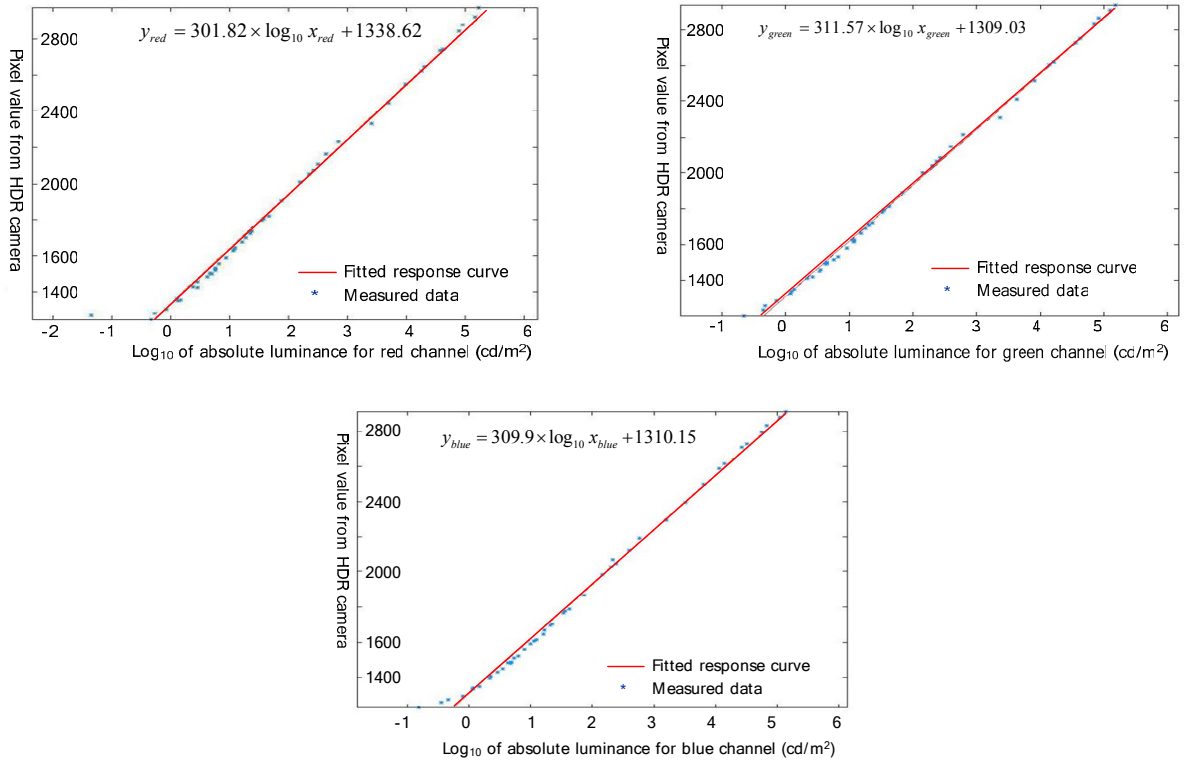

Fig. 6 Absolute response curve: red channel (top left), green channel (top right), blue channel (bottom center)

5. VERIFICATION

Firstly, we test the reciprocity using the Spectralon white reference for checking the stability and the accuracy of our system. We measure the BRDF of several material samples of different color and/or surface characteristics to demonstrate the accuracy of our system. Finally, we make comparison between our proposed system and an existing image-based BRDF measurement system to validate the efficiency.

5.1. Reciprocity

The reciprocity principle states that the BRDF should be the same if the angles of incidence and reflection are interchanged. It is one of the important BRDF features[2] and is tested using the Spectralon white reference. We measure the reflected light from the Spectralon sample to check the reciprocity instead of using spherical sample to check the accuracy of the proposed system. We compare the absolute intensity from the HDR camera for each channel of R, G, B. We tested 40 samples for the reciprocity check. Table 2 shows six representative reciprocity check results which include

the retro-reflection and near grazing angles. It shows that reciprocity is satisfied within 5 % for all angles as great as 85 degree from the surface normal.

Table. 2 Reciprocity check on the Spectral white reference using our BRDF measurement system

θ_i	θ_r	Pixel values			Absolute values			Absolute value/cosθ_i			Error (%)		
		R	G	B	R	G	B	R	G	B	R	G	B
0	3.5	1808.1	1793.9	1774.3	35.9	36.0	31.5	35.9	36.0	31.5	1.5	0.8	1.5
3.5	0	1805.8	1792.5	1772	35.3	35.6	30.9	35.4	35.7	31.0			
12	14	1791.2	1780.7	1758.6	31.6	32.7	28.0	32.3	33.4	28.6	0.1	0.3	0.2
14	12	1790.2	1779.2	1757.3	31.4	32.3	27.7	32.3	33.3	28.6			
25	32	1779.5	1765.6	1745.6	28.9	29.2	25.4	31.9	32.2	28.0	0.5	1.3	0.6
32	25	1770.2	1758.4	1735.9	26.9	27.7	23.7	31.7	32.6	27.9			
36	60	1755.9	1741.9	1720.6	24.1	24.5	21.1	29.8	30.3	26.1	3.2	2.4	1.4
60	36	1688.6	1673.6	1654.0	14.4	14.8	12.9	28.9	29.6	25.7			
60	70	1715.1	1700.7	1676.0	17.7	18.1	15.2	35.3	36.1	30.3	2.8	2.5	0.2
70	60	1661.7	1645.9	1625.2	11.8	12.1	10.4	34.3	35.2	30.3			
82	84	1816.6	1800.7	1774.2	38.4	37.9	31.4	274.2	270.6	224.7	3.4	2.8	3.3
84	82	1744.9	1758.5	1731.4	27.9	27.7	22.9	264.2	270.6	224.7			

5.2. Measurement of isotropic materials

We measure BRDF data of four sample materials having isotropic reflectance property such as glossy blue, green plastics, gold coated metal and gold metallic paint for various incident angles.

Fig. 7 (a) shows the BRDF measurements of the glossy blue plastic at $\theta_i = 2°, 30°$ and $60°$ for each channel of R, G, B. Except for the specular peak, the diffuse reflection is nearly constant. The diffuse reflection gives the material its blue color since it is dependent on the wavelength. On the contrary to the diffuse reflection, the specular reflection of glossy blue plastic gives the specular peak area as white color since it is not dependent on the wavelength. The specular peaks of each measurement appear near the mirror reflection angle due to the glossy-like component of surface reflection and show a very narrow specular lobe.

The measured BRDF of glossy green plastic is shown in Fig. 7 (b). Similar to the glossy blue plastic, it shows a nearly diffuse reflection and also gives a very narrow specular lobe. The specular peaks of each measurement ($\theta_i = 2°, 15°, 30°, 45°, 60°, 70°, 80°$) appears near the mirror reflection angle. As the incidence angle increases, the magnitude of BRDF also increases due to Fresnel property[2].

Fig. 7 (c) shows the measured BRDF of gold coated metal. The gold coated metal shows a weak diffuse reflection in contrast to the two plastics that show nearly diffuse reflection. But similar to the two plastics, the magnitude of BRDF is increases as the incidence angle ($\theta_i = 2°, 15°, 30°, 45°, 60°, 70°, 80°$) increases. We can clearly observe the off-specular phenomenon[28] at $\theta_i = 60°$. As the incident angle increases, the off-specular phenomenon must be amplified. But we cannot observe the amplification of the off-specular phenomenon due to the lack of BRDF samples near the grazing angle.

As shown in Fig. 7 (d), the gold metallic paint scatters light through a more complex mechanism than the gold coated metal and two plastics since the reflection depends upon many factors including the layer thickness, the volume density, the orientation and the size of aluminum flakes, as described in Ershov's work[29]. It shows an unstable diffuse reflection due to the sparkling effect of the aluminum flakes. Similar to the gold coated metal, the gold metallic paint also shows a weak diffuse reflection. On the contrary to the gold coated metal, two specular lobes exist in the gold metallic paint, as explained in the HTSG model[6]. The first specular lobe occurs due to subsurface scattering. The light reflection from the clear coat layer generates the second specular lobe, as described by Günther's research work[30]. As the incident angle ($\theta_i = 10°, 30°, 60°, 70°, 80°$) increases, we can clearly observe the amplification of the second lobe of the gold metallic paint.

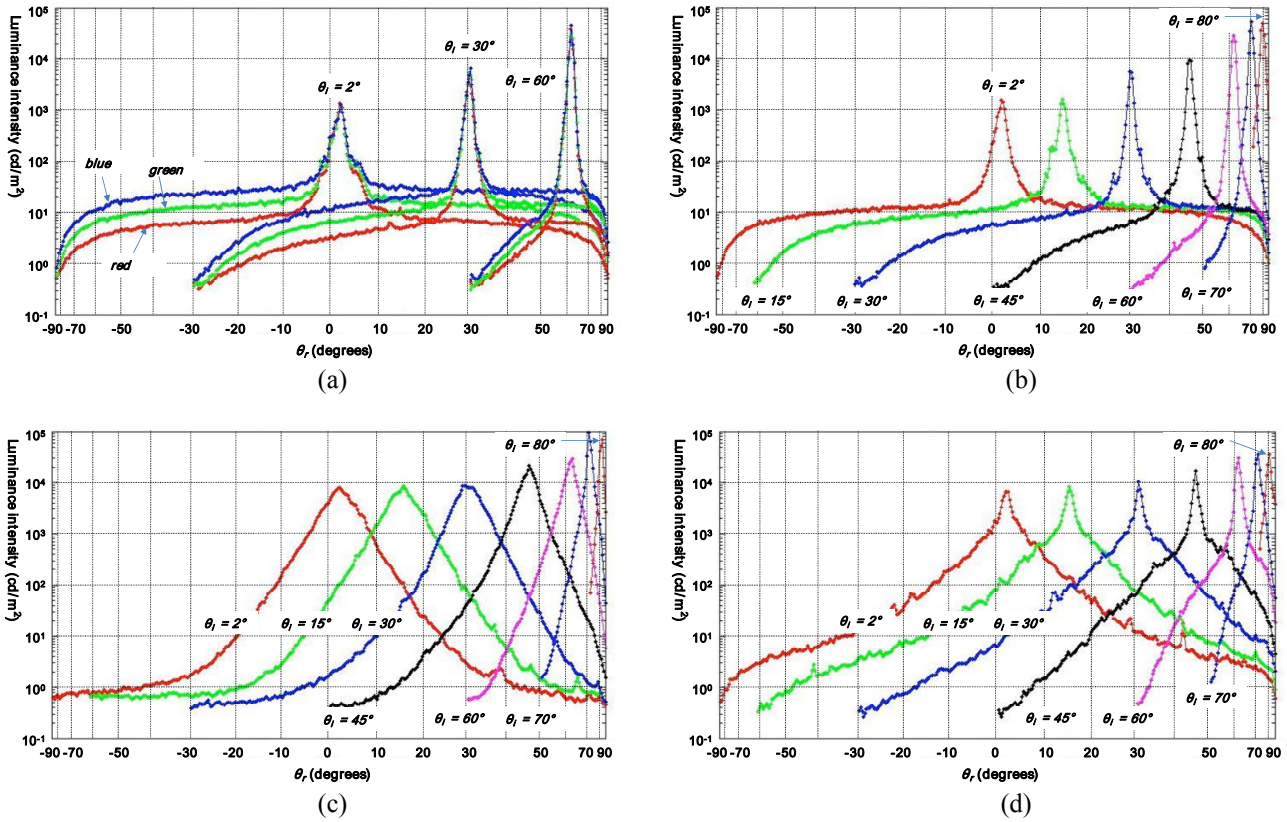

Fig. 7 Measured BRDF data for various incident angles: glossy blue plastic (a) for R,G,B channel, of glossy green plastic (b) for G channel, gold-coated metal (c) for R channel, and gold metallic paint (d) for R channel.

5.3. Comparison with the LDR-based BRDF measurement system

We compare the capability of our proposed system with Matusik's [18] which consists of a light source, a digital camera and a spherical sample. The Matusik's system takes several hours to acquire the full BRDF data. The raw data generated from the Matusik's system becomes about 5 GB when the data is collected at every one degree. Our proposed system can acquire the full BRDF of one material sample in 90 seconds. In addition, the light source can move in an increment of 0.1 degree from 3.5 degree to 173 degree. The comparison between our proposed system and the LDR-based system is shown in Table 3.

Table. 3 Comparison between our proposed HDR-based system and Matusik's system

Contents	Our proposed system	Matusik's system
Image resolution of raw data	640×480	1300×1030
Angular resolution	0.1 degree	0.5 degree
HDRI File size for each direction	0.95 MB (one HDR image)	30 MB (18 different exposure images)
Total file size of raw data	161.5 MB (for 1 degree) 1.61 GB (for 0.1 degree)	4.95 GB (for 1 degree) 49.5 GB (for 0.1 degree)
Angular coverage range	3.5~173 degrees	165 degrees
Total acquisition time	90 seconds	4 hours

6. RENDERING RESULT

We demonstrate the use of measured data by rendering 3D objects with it. We apply the BRDF data of different materials to the Stanford bunny and Venus model, as shown in Fig. 9 and 10. Fig. 8 shows the photographs of real material samples. We observe through visualization that the measured BRDF data generated from our proposed system produces accurate rendering results.

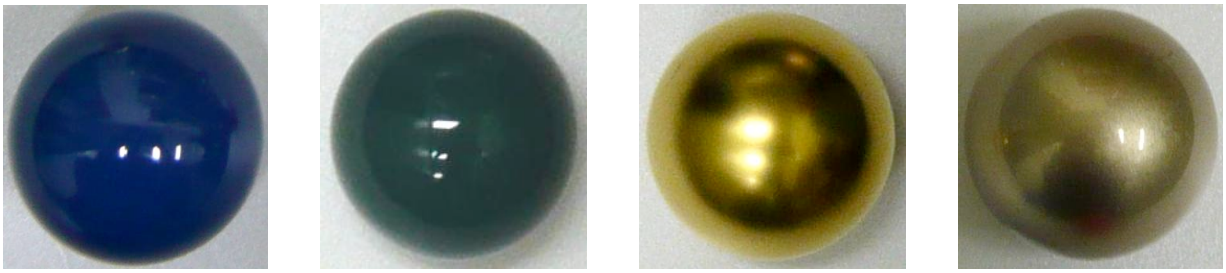

Fig. 8 Four isotropic materials:, glossy blue, green plastic, gold coated metal, gold metallic paint

Fig. 9 Rendering results of Stanford bunny at $\theta_i = 15°$: glossy blue, green plastic, gold coated metal, gold metallic paint

Fig. 10 Rendering results of Venus model at $\theta_i = 15°$: glossy blue, green plastic, gold coated metal, gold metallic paint

7. CONCLUSION AND FUTURE WORK

We present a fast and accurate image-based BRDF measurement system for isotropic reflection materials. It also provides a wide angular coverage and noise reduction capability so that it achieves accuracy that is needed for various applications. Our system can measure real material samples in 90 seconds even with 0.1 degree sampling density. The system covers a wide angular range with the exception of 3.5 degree around retro-reflection to 173 degree, the near grazing angle. We reduce the noise during BRDF data acquisition and processing by using a well furnished dark room and performing photometric calibration. We validate the system in many ways such as checking the uniformity of light source, checking light constancy over time, and checking reciprocity. We demonstrate the capability of the system by producing photorealistic images using the measured BRDF data of different material samples.

We achieve the quality of rendering results comparable to the image-based BRDF measurement system using an LDR camera but with much greater speed and angular resolution. Being compared with the previous image-based BRDF measurement system, our proposed system can provide much faster operation since the HDR camera can acquire approximately 8 orders of luminance magnitude at once. It also performs a quick photometric calibration since it recovers a radiance map from one HDR image while the previous image-based systems take 12 to 18 multiple exposure images to recover the radiance map.

Our system measures the isotropic reflection materials. However, it can be extended to measure anisotropic reflection materials by rotating the cylindrical sample which is wrapped with stripes of the material at different orientations, as described by Ngan[32]. We also plan to extend our system to measure materials with highly specular surfaces.

ACKNOWLEDGEMENTS

This research is supported by the Korea Science and Engineering Foundation (KOSEF) through the National Research Laboratory Program funded by the Korea government (MEST) (No. R0A-2007-000-20049-0) and the CTI development project, MCT and KOCCA in S. Korea.

REFERENCES

1. D. P. Greenberg, K. E. Torrance, F. X. Sillion, J. Arvo, J. A. Ferwerda, S. Patanaik, E. P. F. Lafortune, B. Walter, S. C. Foo, and B. Trumbore, “A framework for realistic image synthesis,” Comput. Graph. Proc. Ann. Conf. Series (SIGGRAPH97), pp. 477-494, (1997).
2. F. E. Nicodemus, J. C. Richmond, J. J. Hsia, I. W. Ginsberg, and T. Limperis, “Geometrical Considerations and Nomenclature for Reflectance,” National Bureau of Standards, (1977).
3. B. T. Phong, “Illumination for computer generated pictures,” Communications of ACM, 18(6), pp.311-317, (1975).
4. J. F. Blinn, “Models of light reflection for computer synthesized pictures,” In Proceedings of the 4th annual conference on Computer graphics and interactive techniques, pages 192-198. ACM Press, (1977).
5. R. L. Cook and K. E. Torrance, “A reflectance model for computer graphics,” ACM Trans. Graph., 1(1), pp. 7-24, (1982).
6. X. D. He, K. E. Torrance, F. X. Sillion, and D. P. Greenberg, “A comprehensive physical model for light reflection,” In Proceedings of the 18th annual conference on Computer graphics and interactive techniques, pp. 175-186, (1991).
7. J. F. Murray-Coleman and A. M. Smith, “The Automated Measurement of BRDFs and their Application to Luminaire Modeling”, Journal of the Illuminating Engineering Society, pp. 87-99, (1990).
8. J. E. Proctor, P. V. Barnes, “NIST high accuracy reference reflectometer-spectrophotometer,” J. Res. Natl. Inst. Stand. Technol. 101, pp. 619-627, (1996).
9. D. R. White, P. Saunders, S. J. Bonsey, J. van de Ven, and H. Edgar, “Reflectometer for measuring the bi-directional reflectance of rough surfaces,” Appl. Opt. 37, pp. 3450-3454, (1998).
10. H. Li, S. C. Foo, K. E. Torrance, S. H. Westin, “Automated three-axis gonioreflectometer for computer graphics applications,” Optical Engineering 45(4), pp. 1-10(043605), (2006).
11. G. J. Ward, “Measuring and modeling anisotropic reflection,” Comput. Graph., 26, pp. 265-272, (1992).
12. K. Dana “BRDF/BTF Measurement Device,” Proceedings of the IEEE International Conference on Computer Vision, 2, pp. 460-466, (2001).

13. Y. Mukaihawa, K. Sumino, Y. Yagi, “High-speed measurement of BRDF using an ellipsoidal mirror and projector,” Proceedings of the IEEE Computer Society Conference on Computer Vision and Pattern Recognition, (2007).
14. J. Gu, C. Tu, R. Ramamoorthi, P. Belhumeur, W. Matusik and S. K. Nayar, "Time-varying Surface Appearance: Acquisition, Modeling, and Rendering", ACM Trans. Graph., 25(3), pp. 762-771, (2006).
15. M. Ben-Ezra, J. Wang, B. Wilburn, X. Li, and L. Ma, “An LED-only BRDF Measurement Device,” to appear in the IEEE Conference on Computer Vision and Pattern Recognition (2008).
16. K. F. Karner, H. Mayer, and M. Gervautz, “An image based measurement system for anisotropic reflection,” Comput. Graph. Forum 15, pp. 119-128, (1996).
17. S. R. Marschner, S. H. Westin, E. P. F. Lafortune, and K. E. Torrance, “Image-based bidirectional reflectance distribution function measurement,” Appl. Opt. 39, pp. 2592-2600, (2000).
18. W. Matusik, H. Pfister, M. Brand, and L. McMillan, “A Data driven Reflectance Model,” ACM Trans. Graph., 22(3), pp. 759-769, (2003).
19. Günther J., Chen T., Goesele M., Wald I., and Seidel H. P., “Efficient Acquisition and Realistic Rendering of Car Paint,” In Proc. Vision, Modeling, and Visualization, pp. 487–494, (2005).
20. M. R. Chowdhury, K. Y. Kim, H. J. Yoo, H. M. Kim, M. K. Seo and K. H. Lee, “Realistic material Modeling for Product Design,” Design Engineering Workshop, 7th IJCC Japan-Korea CAD/CAM Workshop, pp. 104-107, (2007).
21. S. B. Kang, M. Uyttendaele, S. Winder, and R. Szeliski, “High Dynamic Range Video,” ACM Transactions on Graphics (Proceedings of SIGGRAPH 2003), 22(3), pp. 319-325, (2003).
22. M. A. Robertson, S. Borman, and R. L. Stevenson, “Estimation-Theoretic Approach to Dynamic Range Enhancement using Multiple Exposures,” J. Electronic Imaging, 12(2), pp. 219-285, (2003).
23. T. Lule, H. Keller, M. Wagner, and M. Bohm, “LARS II - A High Dynamic Range Image Sensor with a-Si:H Photo Conversion Layer,” In 1999 IEEE Workshop on Charge-Coupled Devices and Advanced Image Sensors, Nagano, Japan, (1999).
24. G. Krawczyk, M. Goesele, H. P. Seidel, "Photometric Calibration of High Dynamic Range Cameras," MPI-I-2005-4-005, May (2005).
25. M. Goesele, H. P. A. Lensch, W. Heidrich, and H. P. Seidel, “Building a Photo Studio for Measurement Purposes,” In Proceedings of VMV'00, pp. 231-238, (2000).
26. T. J. Papetti, W. E. Walker, and C. E. Keffer, B. E. Johnson, “MRDF and BRDF measurements of low-scatter materials,” Proceedings of SPIE – Vol. 6550, Laser Radar Technology and Applications XII, (2007).
27. R. Y. Tsai, “A Versatile Camera Calibration Technique for High-Accuracy 3D Machine Vision Metrology Using Off-the-shelf TV Cameras and Lenses,” IEEE JOURNAL OF ROBOTICS AND AUTOMATION, VOL. RA-3, NO. 4, AUGUST (1987).
28. K. Torrance and E. Sparrow, “Theory for Off-Specular Reflection from Rough Surfaces,” Journal of the Optical Society of America, 57(9), pp. 1105-1114, (1967).
29. S. Ershov, R. Durikovic, K. Kolchin, K. Myszkowski, “Reverse engineering approach to appearance-based design of metallic and pearlescent paints,” The Visual Computer, vol. 8-9, No.20, pp. 586-600, (2004).
30. J. Günther, T. Chen, M. Goesele, I. Wald, and H. P. Seidel, “ Efficient Acquisition and Realistic Rendering of Car Paint,” In: Vision, Modeling, and Visualization 2005 (VMV'05), pp. 487-494, 2005
31. R. S. Berns, “principles of color technology 3rd ed.,” John Wiley and Sons, Inc., (2000).
32. A. Ngan, F. Durand, and W. Matusik, “Experimental analysis of BRDF models,” In Proceedings of the 16th Eurographics Symposium on Rendering, pp.117-126, (2005).